E1-2001-36

ANALYZING POWERS OF INELASTIC *dp*-SCATTERING IN THE ENERGY REGION OF DELTA AND ROPER RESONANCES EXCITATION

Submitted to «Physical Review C»

L.V.Malinina[1], G.D.Alkhazov[2], W.Augustyniak[3], M.Boivin[4], J.-L.Boyard[5], R.Dahl[6], M.Drews[6], C.Ellegaard[6], L.Fahri[5], C.Gaarde[6], T.Hennino[4,5], J.C.Jourdain[5], M.Kagarlis[4], A.V.Kravtsov[2], R.Kunne[4,5], J.S.Larsen[6], P.Morsch[7], V.A.Mylnikov[2], E.M.Orichtchin[2], C.F.Perdrisat[8], N.M.Piskunov, A.N.Prokofiev[2], V.Punjabi[9], P.Radvanyi[4,5], B.Ramstein[5], B.V.Razmyslovich[2], M.Roy-Stephan[5], I.M.Sitnik, M.Skousen[6], E.A.Strokovsky, I.I.Tkach[2], E.Tomasi-Gustafsson[4,10], S.S.Volkov[2], A.A.Zhdanov[2], P.Zupranski[3]

[1]E-mail: malinina@sunhe.jinr.ru
[2]PNPI, 188300, Gatchina, Russia
[3]Andrzej Soltan Institute for Nuclear Studies, Warsaw, Poland
[4]LNS, CEA/DSM and CNRS/IN2P3, CE Saclay, 91191 Gif-sur-Yvette Cedex, France
[5]IPN CNRS/IN2P3 and Universite Paris-sud, 91400 Orsay, France
[6]Niels Bohr Institute, Copenhagen, Denmark
[7]KFZ-Juelich, D-52425 Juelich, Germany
[8]The College of William and Mary, Williamsburg, Virginia 23185, USA
[9]Norfolk State University, Norfolk, Virginia 23504, USA
[10]CEA/DAPNIA/SPhN, CE Saclay 91191 Gif-sur-Yvette Cedex, France

I. INTRODUCTION

The excitation of broad hadronic resonances in nuclei by isoscalar projectiles has been studied intensively in recent years [1] – [5]. The inelastic interaction of isoscalar projectiles (as α or d) with a proton holds the prospect of isolating isobar excitations according to their isospin. The simplest process is the one where the target is excited to an isobar which then must have I=1/2; it must occur through isoscalar meson exchange. There is also the possibility that the excitation occurs in the projectile through exchange of an isoscalar or an I=1 meson, in the latter case the Δ can also contribute (Fig. 1).

The interest of a study of the $N^*(1440)$, the Roper resonance, excitation by isoscalar projectiles was revived several years ago, following the observation of isospin 1/2 excitation of the proton in the region of the Roper resonance $N^*(1440)$ in the inclusive $p(\alpha,\alpha')X$ [4] and in $p(d,d')X$ reactions [5]. The contribution to the total cross section of inelastic (α,α') and (d,d') scattering from the amplitude corresponding to Δ excitation is large at energies of several GeV. Therefore, analysis of these processes in terms of the Roper resonance excitation is not free from ambiguities. The deuterons, conserving all advantages of the isoscalar projectile, are spin-one particles; therefore, using a polarized deuteron beam one can study polarization effects and obtain new information about the hadronic resonances excitation.

The simplest polarization observable for $p(d,d')X$ is the tensor analyzing power A_{yy}. It was measured inclusively in Dubna and in Saclay in 1993-1994 [6], [7]. The experimental data show that it increases with increasing of $|t|$ almost linearly up to $|t| \simeq 0.3$ (GeV/c)^2 and decreases at higher $|t|$. Such a behavior of the tensor analyzing power is fairly well reproduced in the theoretical framework of the exchange of ω meson in an algebraic collective model used for the electroexcitation of nucleon resonances [8],[9]. In that approach the tensor analyzing power is expected to be very sensitive to the isoscalar longitudinal form factor of the Roper resonance excitation, while the others low mass nucleon resonances $S_{11}(1535)$, $D_{13}(1520)$ and $S_{11}(1650)$ have only isovector longitudinal form factors [9]. This specific property of the Roper resonance combined with the t dependence of the deuteron form factors determines the t behavior of the tensor analysing power A_{yy}. An attempt to analyze the experimental data for the inclusive $p(d,d')X$ reaction in the framework of this model has been done in [10].

A guiding idea of present experiment was that by comparing single and double pion final states, one could distinguish the two reaction channels further. Indeed the free Δ does not decay into two pions final state, whereas the N* resonances do. Selecting 2-pion events would have the effect of eliminating I=3/2 projectile excitation contributions.

In this article we present data for the tensor and vector analyzing powers in dp inelastic scattering at kinetic energy T_d = 2430 MeV, what is very close to the $N^*(1440)$ excitation threshold ($\sim$ 30 MeV in the NN c.m.s.) [1]. The scattered deuterons were registered at angles close to 0.4^o. The kinematic of the $dp \to d'X$ reaction was almost collinear. The exclusive experiment was performed at the SATURNE-II accelerator with the SPES4-π setup. The experimental data contain information about the following channels of the inelastic deuteron scattering on protons:

$$dp \to dp\pi^0 \tag{1}$$

$$dp \to dn\pi^+ \tag{2}$$

$$dp \to dN\pi\pi \tag{3}$$

[1]Deuteron is a weekly bound state so mainly only one of its nucleons participates in the interaction. In pp ($p_p = p_d/2$) kinematic, T_p =1215 MeV: $T^{threshold}_{pp\to pN^*}$ = 1138 MeV. In dp, T_d = 2430 MeV: $T^{threshold}_{dp\to dN^*}$ =1620 MeV.

The channels with one pion in the final state can occur both from the Δ and from the N^* resonance decays:

$$d + p \to d + N^*(1440), \quad N^* \to p + \pi^0$$
$$d + p \to d + N^*(1440), \quad N^* \to n + \pi^+$$
$$d + p \to d^* + p, \quad d^* \to d + \pi^0$$
$$d + p \to d^* + n, \quad d^* \to d + \pi^+$$

where d^* is the scattered deuteron with one of its nucleons excited in Δ state. It can result in an interference effects in the region of the resonance overlapping.

The tensor and vector analyzing powers for different channels of (d, d') reaction have been measured as functions of the squared deuteron 4-momentum transfer t, or the effective mass of the binary subsystem $(N\pi)$ (see Fig. 2), and the pion emission angle in the reaction plane relative to incident deuteron momentum. The kinematical region for $d + p \to d + X$ reaction in the $(t - M_x)$ plane studied in this experiment is shown in Fig. 2.

II EXPERIMENTAL SETUP

The SPES4-π setup which was used in a series of experiments at SATURNE-II is shown in Fig. 3. It consists of a large acceptance non-focusing magnetic spectrometer (magnet Tethys and detectors: Forward (FS) and Lateral (LS) spectrometers) in combination with the high resolution focusing magnetic spectrometer SPES4 [11]. Below we shall confine our consideration to the Forward spectrometer only (described in detail in [12]), since the LS information was not used in the present analysis. The particles of high momenta (in this experiment: d') were detected in SPES4 while the secondary low momentum charged particles (protons and pions from the reactions listed above) were detected in the non-focusing magnetic spectrometer FS.

SPES4. The SPES4 spectrometer is about 33 meter long and consists of four dipoles, six quadrupoles and a correcting sextupole. Two scintillation hodoscopes I and F are located at the intermediate and the final foci, respectively. The hodoscope in the intermediate focus I consists of a row of scintillation counters while F consists of two rows of overlapping counters. The following combinations of the signals from scintillation counters were used for the trigger: SPES4= $(I_i \cap F_i) \cup (I_i \cap F_{i+1})$, where i is the counter number. Two 2-cm thick scintillators (ΔE-detector) were placed after the hodoscope F to measure the detected particle ionization loss. Usually two drift chambers (with four wire planes each) placed before the F-hodoscope were used for the momentum reconstruction of scattered particle, but in this experiment these chambers were not used and the deuteron momentum was reconstructed from the F-counter numbers; the resulting momentum resolution was $\simeq 0.4\%$ [13].

Particles were identified by time of flight and energy loss in the ΔE-detector. This information was used to separate deuterons from background protons from the elastic $dp \to pd$ backward scattering.

The angular acceptance of the spectrometer was $\sim 3 \times 10^{-4}$ sr.

In this experiment the outgoing beam was trapped after the first dipole of SPES4 by a 50 cm thick lead beam stopper. The directions of the outgoing beam and of the particle detected in SPES4 were separated no more than 1^o at the entrance of SPES4.

Tethys. The analyzing magnet Tethys was one of the two magnets that formed earlier the CERN split field magnet. Its horizontally oriented pole face has the shape of a square with a side of 100 cm; the pole aperture is 50 cm. The magnet was oriented with its iron yoke in the direction of the incoming beam: a hole of 20 cm width and 10 cm height provided a free path for the beam inside the magnet. Placed on air cushions, the magnet could be rotated around a fixed point, thus permitting the alignment of the entry hole with the direction of the incoming

beam. The latter could be varied, thus allowing the selection of that part of the angular domain of the reaction which one wanted to study. The 6 cm long liquid hydrogen (LH) target was placed in the magnetic field approximately 25 cm after the entry hole.

The vertical component of the magnetic field was measured at three field strengths (6, 9, 12 kG), both in the median plane and in the plane 15 cm above the median plane. From the measured field values, a 3-dimensional field map was constructed and extrapolated to a surface 4×3.7 m^2 [14]. In this experiment three maximal values of the magnetic field were used: 7.892, 8.142, 8.418 KG, corresponding to three central momenta of the SPES4 2.85, 2.94, 3.04 GeV/c respectively.

The Forward Spectrometer. The Forward spectrometer (FS) was designed and built by the St. Petersburg Nuclear Physics Institute group. The FS consisted of six drift chambers ($X1, Y1, U, V, Y2, X2$) and a scintillator hodoscope placed behind the chambers. It was used for triggering and for particle identification. The $X1$ and $X2$ coordinates defined the intersections of the charged particle trajectory with the chamber planes in the horizontal direction, and the $Y1$ and $Y2$ coordinates in the vertical one; in addition U and V planes, with wires inclined by an angle of about $\pm 10^o$ to the vertical axis, helped resolve many-particle ambiguities. The active area of the planes varied from 0.5×1.2 m^2 ($X1, Y1$) to 0.7×1.7 m^2 ($X2, Y2$). The scattered deuterons as well as the unscattered beam passed through a hole in each of the FS chambers and the FS hodoscope into the SPES4 entrance. The size of these holes was about 10×13 cm^2 in the chambers and 20×30 cm^2 in the hodoscope. Particles detected in the FS were identified by the time of flight and the energy loss in the hodoscope.

The procedure of alignment of the FS and the momentum reconstruction algorithm are described in [13],[14].

The beam and monitors. The deuteron beam polarization was changed in the usual burst-to-burst mode; states 5, 6, 7, 8 (in SATURNE-II notations, see Table I), were used. The sum of states "5+6"("7+8") gives positive (negative) tensorially polarized beam without vector polarization admixture.

Table I. Maximum values of the beam vector and tensor polarization parameters for used beam polarization states at Saturne-II (taken from [19]).

Number of the beam polarization state	P_{ZZ}^{max}	P_{Z}^{max}
5	+1	+1/3
6	+1	−1/3
7	−1	+1/3
8	−1	−1/3

The sum of "5+7"("6+8") gives positive (negative) vectorially polarized beam without tensorial admixture . The combinations "5+8" and "6+7" give unpolarized beam. The vector polarization was normal to the plane containing the mean beam orbit of the accelerator. The beam polarization was measured periodically during the experiment with the SATURNE-II Low-Energy polarimeter. The average beam polarizations were $P_{ZZ} = 0.902 \pm 0.015$ and $P_Z = 0.311 \pm 0.008$ and $|P_Z^+| = |P_Z^-|$ ($|P_{ZZ}^+| = |P_{ZZ}^-|$).

The beam intensity was typically $I \simeq 10^6$ deuterons/spill. It was monitored by three independent monitors:

• a relative monitor, consisted of two independent detector arms each consisting of a telescope of three small scintillation counters. Particles knocked out from a 250 mkm Ta foil placed in the beam 5 m upstream the LH target were detected by each of arms independently.

• secondary emission chamber (CES). The beam traversed a metal foil, and the created free electrons were collected on an anode. The number of secondary electrons is proportional to the beam intensity.
• a scintillation counter (SBEAM), operating at lowered voltage, which was placed in the direct incoming beam just before the hole in the Tethys yoke; the thickness of this scinitllator was about 0.5 cm.

These methods gave the relative beam intensity, but it was checked that they are consistent with each other. In data analysis the relative beam intensity measured by SBEAM was used because of the highest counting rate of this monitor, provided a minimal statistical errors being so important in the polarization measurements. Its counting rate was found to be proportional to the beam intensity. It was checked periodically by the measurement of the activation of the thin carbon target inserted in the beam during 10 minutes. The ratios of the counting rates of this monitor to the other ones were verified to be constant for all bursts used in the data analysis.

III MEASURED QUANTITIES

The main goal of the present experiment was the measurement of the analyzing powers A_{yy} and A_y for reactions (1)-(3). Following the Madison convention [15], a Cartesian coordinate system was used with the z-axis along the incident beam, the y-axis normal to the scattering plane (and parallel to the direction of the incident deuteron spin quantization axis), the x- axis defined a right-handed coordinate system. The cross-section of the dp inelastic scattering can then be written as :

$$\sigma^{\pm}(\theta_\pi, t) = \sigma^0(\theta_\pi, t)[1 + \frac{3}{2}P_Z{}^{\pm}A_y(\theta_\pi, t) + \frac{1}{2}P_{ZZ}{}^{\pm}A_{yy}(\theta_\pi, t)], \tag{7}$$

where σ^0 and $\sigma^{\pm}$ are the cross-sections for unpolarized and polarized beam; "+", "−", "0" denote the corresponding beam polarization; $A_y(\theta_\pi, t)$ and $A_{yy}(\theta_\pi, t)$ are the vector and tensor analyzing powers of the reaction; θ_π is the horizontal pion emission angle, t is the deuteron 4-momentum transfer squared; $P^{\pm}_{ZZ}$ and $P^{\pm}_Z$ are the beam polarizations where Z is related to the polarized deuteron source coordinate system [15].

It is easy to solve equation (7) using the combination of the polarization states with tensorially polarized beam without vector polarization admixture and the vectorially polarized beam without tensor polarization admixture if $|P^+_Z| = |P^-_Z|$ ($|P^+_{ZZ}| = |P^-_{ZZ}|$):

$$A_{yy}(\theta_\pi, t) = \frac{2}{P_{ZZ}} \cdot \frac{\sigma^+{}_t - \sigma^-{}_t}{\sigma^+{}_t + \sigma^-{}_t} \tag{8}$$

$$A_y(\theta_\pi, t) = \frac{2}{3P_Z} \cdot \frac{\sigma^+{}_v - \sigma^-{}_v}{\sigma^+{}_v + \sigma^-{}_v} \tag{9}$$

where $\sigma^{\pm}{}_{t,v}$ are the cross-sections for the tensorially (vectorially) polarized beam.

In this experiment the tensor A_{yy} and vector A_y analyzing powers were calculated for each selected reaction by the following way:

$$A_{yy}(\theta_\pi, t) = \frac{2}{P_{ZZ}} \cdot \frac{N_5 + N_6 - N_7 - N_8}{N_5 + N_6 + N_7 + N_8} \tag{10}$$

$$A_y(\theta_\pi, t) = \frac{2}{3P_Z} \cdot \frac{N_5 - N_6 + N_7 - N_8}{N_5 + N_6 + N_7 + N_8} \tag{11}$$

$$A_0(\theta_\pi, t) = \frac{N_5 - N_6 - N_7 + N_8}{N_5 + N_6 + N_7 + N_8} \ . \tag{12}$$

Here N_5, N_6, N_7 and N_8 are the numbers of events detected at each beam polarization state normalized to the corresponding beam intensities.

The last equation represents the false asymmetry. This asymmetry was checked for all reaction channels and was consistent with zero in all cases, proving that the polarization observables were under full control.

IV MEASUREMENTS

The measurements were done at the deuteron beam momentum 3.73 GeV/c with three different settings of the SPES4 and Tethys magnetic fields, to assure a complete coverage of the Roper resonance mass region (Fig. 4). The central momentum settings of the SPES4 spectrometer were 2.85 GeV/c, 2.94 GeV/c and 3.04 GeV/c. The corresponding regions of the 4-momentum transfer squared t were: for 2.85 GeV/c $-0.28 \leq t \leq -0.14$, for 2.94 GeV/c $-0.22 \leq t \leq -0.1$, for 3.04 GeV/c $-0.17 \leq t \leq -0.07$. The Tethys and SPES4 magnetic fields were varied proportionally, assuring identical trajectories of the deuterons accepted by SPES4. The field strengths were monitored by use of NMR probe with accuracy better than 1 Gauss.

The coincidences of signals from SPES4 (see above) and the scintillation hodoscopes of the FS were used for the trigger: SPES4 $\cap$ (FS $\cup$ LS).

For each setting background measurements with the empty target were performed periodically. The "full" to "empty" event ratio, after all selection criteria were applied, amounted to $\simeq 20$.

The summary of the main characteristics of the setup and the data taking is given in Table II.

Table II. Experimental and setup parameters.

Forward Spectrometer	
Coordinate resolution σ	~ 0.3 mm
Momentum resolution $\delta p/p$	$\sim 5\%$
Horizontal angular resolution $\delta\theta_x$	~ 0.02 rad
Vertical angular resolution $\delta\theta_y$	~ 0.0014 rad
SPES4	
Momentum resolution $\delta p/p$	0.4%
Angular acceptance	3×10^{-4} sr
Momentum acceptance $\Delta p/p$	$\pm 4\%$
Horizontal angular acceptance $\Delta\theta_x$	(–0.0135 , 0.0185) rad
Vertical angular acceptance $\Delta\theta_y$	± 0.0114 rad
Beam and experimental parameters	
Trigger	SPES4 $\cap$ (FS $\cup$ LS)
Missing mass resolution in the nucleon mass region	~ 20 MeV/c^2
Full/empty target ratio for selected events	~ 20
Deuteron beam momentum:	3.73 GeV/c
Average beam polarization P_{ZZ}	0.902 ± 0.015
Average beam polarization P_Z	0.311 ± 0.008
Beam polarization control	Low energy polarimeter d(d,p)t , $E_d = 400$ KeV
Average beam intensity	$\sim 10^6$/spill
Liquid hydrogen target dimensions	length 6 cm ; diameter 3 cm

V DATA ANALYSIS AND RESULTS

Identification of the reaction channels

The detected events originated mainly from the inelastic $p(d,d')N\pi(\pi)$ reaction and elastic backward $p(d,p)d$ scattering [16], as seen in Fig. 5. The elastic process was unambiguously identified by detecting the recoil proton in SPES4 ($p_p \simeq 2.93$ GeV/c) in coincidence with the scattered deuteron in the FS ($p_d \simeq 0.8$ GeV/c). It provided useful information for the calibration of the setup [14], [13]. The data on the $p(d,p)d$ tensor analyzing power, obtained in the present experiment and published in [16], agree very well with the existing world data [17], [18]. For the inelastic process $p(d,d')X$, $X = N\pi(\pi)$, the scattered deuterons were detected by SPES4, while the charged products of the decay of the intermediate system X were registered by the forward spectrometer.

The calculated missing mass was used for the identification of the reaction channels:

$$m_x{}^2 = (P_d + P_{target} - P'_d - P_{ch})^2,$$

where $P_{ch} = (E_{ch}, \vec{p}_{ch})$ is the 4-momentum of the charged particle detected in the FS, π^+ or proton; $P_{target} = (m_{target}, 0, 0, 0)$. The particles in the FS were identified by time of flight (TOF) and energy loss (ADC) measurements. The two-dimentional plots of the TOF versus the energy loss, TOF versus the particle momentum, ADC versus the particle momentum were constructed for each counter of the FS hodoscope and the selection criteria were chosen separately for each counter and for each setting (see an example of such distributions in Fig. 6) . Note that the probability to misidentify a π^+ as protons or a proton as a π^+ increases with increasing particle momentum. Particles with momenta below 0.7 GeV/c can be identified unambiguously. For particles with momenta above 0.7 GeV/c the possibility of different identification was considered separately by the missing mass calculations.

We analyzed events in which one charged particle was detected by the FS and the scattered deuteron by the SPES4. A specific feature of the experiment was that the secondary particles from different reactions populate different angular and momentum regions. In Fig. 7(b,c,d,e,f) the regions of kinematical variables accepted by the setup for all considered reactions are presented. These regions were mapped with a Monte-Carlo simulation using phase space distributions of the particles, with cuts implied by the setup boundaries and the trigger conditions. The sizes of the FS holes were enlarged in the data analysis in order to eliminate random triggers and were set at 18×13 cm^2 in the chambers and 25×30 cm^2 in the hodoscope.

The choice of the experimental cuts for the channel selection was verified by the Monte-Carlo calculations.

If the particle registered in the FS was identified as a positive pion, the missing mass distribution should have a peak close to the neutron mass corresponding to the $dp \to dn\pi^+$ reaction and a broader structure at higher mass corresponding to the reaction $dp \to dN\pi^+\pi$.

If the particle registered in the FS was identified as a proton then the missing mass distribution should have a peak close to the π^0 mass corresponding to the $dp \to dp\pi^0$ reaction and a broader distribution at higher corresponding to the $dp \to dp\pi\pi$ reaction.

The π^- were not considered due to low acceptance for π^- registration by the FS.

The results of A_{yy} and A_y measurements are presented in Table III. The errors shown there are only statistical.

A. One-pion production channels

$dp \to dn\pi^+$ reaction

Figure 8 shows the selection of events from $dp \to dn\pi^+$ reaction. Positive pions from this

reaction were detected by the FS. For each setting of the SPES4 spectrometer the region of the corresponding 4-momentum transfer squared t was divided into three equal parts (bins). In Fig. 9 the missing mass squared spectra corresponding to the unobserved neutron from $dn\pi^+$ final state are shown for each $|t|$ bin for both tensor polarization states. The corresponding spectra taken with "empty target" measurements were subtracted. The background from misidentification (very small) was fitted by a polynomial and subtracted. Similar spectra were obtained for all three settings of SPES4.

In Fig. 10(a,b,c) the tensor analyzing power A_{yy}, vector analyzing power A_y and the false asymmetry A_0 are presented for this reaction as a function of the mean $|t|$ value of the bin. The regions covered by the SPES4 settings, ($\Delta p_d/p_d = \pm 4\%$) overlapped (Fig. 4), so it is possible to compare the values of the polarization observables measured at different settings of the spectrometer. From Fig. 10(a) one can see that these measurements are consistent, and then the average values of A_{yy} were taken for each $|t|$, Fig. 10(d). A similar method was used for all other reaction channels.

$dp \to dp\pi^0$ reaction

In Fig. 11 the selection of events from the $dp \to dp\pi^0$ channel is shown for the SPES4 spectrometer setting 2.94 GeV/c when protons were detected in the FS. Similar plots were obtained for settings 2.85 GeV/c and 3.04 GeV/c. In Fig. 11(a) the spot near zero missing mass squared corresponds to $dp \to dp\pi^0$ reaction; the other events are from the $dp \to dp\pi\pi$ and from misidentified positive pions from the reaction $dp \to dn\pi^+$. In Fig. 11(b) the two-dimensional distribution of the proton horizontal emission angle (θ_x) and momentum is shown; the rectangle in the lower left corner indicates the selection criteria for the events from the $dp \to dp\pi^0$ reaction. In the bottom part of the Fig. 11 the distributions of the missing mass squared are shown: Fig. 11(c) represents the one without application of the selection criteria, Fig. 11(d) shows the one for protons with $\theta_x < -0.7$ rad and $p_p < 0.5$ GeV/c. A clear signal for π^0 events was selected for this part of the proton spectra.

The calculated range of the accepted proton momenta and angles is shown in Fig. 7(c). It consists of two parts, with $p_p < 0.5$ and $p_p > 0.7$ GeV/c. Only events with momenta $p_p < 0.5$ GeV/c could be identified reliably. For this reaction it was impossible to distinguish the events with momenta $p_p > 0.7$ GeV/c from the strong background of misidentified events; consequently these events were rejected.

In Fig. 10(d,e,f) the tensor analyzing power A_{yy}, vector analyzing power A_y and false asymmetry A_0 are presented. Because of the lack of statistics for this channel, only the mean value of $|t|$ for each setting is taken.

A_{yy} angular and t-dependence for the one-pion channels

In general the amplitude for $dp \to dN\pi$ reaction depends on the momenta and angles of all outgoing particles, but under the kinematical conditions of this experiment, when the scattered deuterons are detected at angles close to 0^o and M_{eff} is directly related with t, the tensor analyzing power A_{yy} is a function of two independent variables only: the horizontal pion emission angle θ_π and t.

$A_{yy}(\theta_\pi, t)$ is presented in Table III as a function of both variables θ_π and t. It is interesting to study the A_{yy} dependence upon θ_π or t separately, integrating over the accepted values of the other variable. The A_{yy} dependencies upon t and on θ_π are presented in Fig. 10(d,h).

Events from the reactions $dp \to dn\pi^+$ and $dp \to dp\pi^0$ detected in the SPES4-π spectrometer populate different regions of pion emission angles θ_π (Fig. 13). The width of the accepted angular region for $dp \to dp\pi^0$ is narrow. On the contrary for the $dp \to dn\pi^+$ channel it is rather broad and can be divided into three equal parts. The mean value of θ_π over the bin was taken. In Fig. 10(h) the dependence of A_{yy} upon θ_π (for positive pion from $dp \to dn\pi^+$ and for neutral pion from $dp \to dp\pi^0$) reactions is presented. Three points for $dp \to dn\pi^+$ and one for $dp \to dp\pi^0$ are

shown. All possible values of $|t|$ are included, which is equivalent to integration over the whole $|t|$-range. It is seen in this figure that the A_{yy} values are almost the same for the points with similar absolute values of θ_π; A_{yy} is an even smooth function of θ_π, as expected.

If we plot A_{yy} as a function of $|t|$ only (which corresponds to the integration over the pion emission angles allowed by the setup, i.e. $-36^o < \theta_{\pi^+} < 6^o$ for $dn\pi^+$ and $6^o < \theta_{\pi^0} < 36^o$ for $dp\pi^0$ final states) the values of A_{yy} for both $dp \to dN\pi$ channels with the same $|t|$ values are essentially different (Fig. 10(d)). This is due to the different θ_π range selected in both cases.

A_y angular and t-dependence for the one-pion channels

Similarly to A_{yy}, the one pion asymmetry, A_y, for $dp \to dN\pi$ shows a strong angular dependence (Fig. 10(g)). It is an odd function of the angle, consistent with 0 at zero pion emission angles. The A_y angular dependence seems to be understood qualitatively if one takes into account that in collinear kinematics (d' are detected at about zero-angle) the reaction plane is determined by the momentum vector of a secondary particle and the incoming beam direction; therefore when they are almost collinear ($\theta_\pi \sim 0$), the reaction plane becomes undefined.

A_y as a function of $|t|$, integrated over the pion emission angles allowed by the setup, has a different signs for the $dp \to dn\pi^+$ and $dp \to dp\pi^0$ channels at the same $|t|$ values (Fig. 10(b,e)). This is a consequence of the different θ_π range selected.

The dependence of A_y on θ_π and t is presented in Table III; for each bin of θ_π the mean value of $|t|$ for the whole setting is given.

B Two-pion production channels

Channels selection

In this experiment the events from the reaction channels with two pions in the final state are selected when either π^+ or proton were detected in the FS. The case when π^- were detected by the FS was not considered due to low acceptance for π^- registration (Fig 7(f)).

In Fig. 8(b) the missing mass squared spectrum for events from $dp \to dN\pi^+\pi^-$ with π^+ detected in the FS is shown. The selection criteria are complementary to those used for $dp \to dn\pi^+$ with pion momentum < 0.5 GeV/c and angle $\theta_\pi < 0$ (see Fig. 4).

A_{yy} and A_y t-dependence for the two-pions channels

In Fig. 12 the tensor analyzing power A_{yy}, vector analyzing power A_y and the false asymmetry A_0 are presented for the two-pion production channels as functions of t. For the experimental conditions of this experiment the scattered deuterons were detected in SPES4 and only one charged particle among the secondaries was detected in the FS. For the reaction $dp \to dN\pi\pi$ it corresponds to the integration over all possible angles of the non-registered particles. From this point of view in both cases, with registration of π^+ or p, there is no defined reaction plane (in contrast with the $dp \to dN\pi$ reactions), and therefore there is no reason to expect a dependence of A_{yy} and A_y on θ_π; moreover the vector analyzing power A_y for these channels is close to zero Fig. 12(b,e).

The data for A_{yy} were obtained in both ways: when π^+ was detected in the FS or when proton was detected in the FS; the results coincide.

C. Comparision of t-dependence of A_{yy} for one- and two-pion production channels

The difference between the tensor analyzing power A_{yy} for the reaction $dp \to dn\pi^+$ and for the channels with two pions in the final state is not significant (Fig. 14 and Table III). They actually differ only at the point with the maximum $|t|$, t=–0.225 (GeV/c)^2. It was expected that two pions final state corresponds to the pure Roper signal, while for one pion final state both resonances (Roper and Δ) give a contribution. In the low $|t|$ region the Δ excitation in the projectile dominates in inclusive $dp \to dX$ (Fig. 4) [5]. The absence of a difference between

A_{yy} for one and two pions final states may be an indication that A_{yy} is affected mostly by the deuteron form factors and that its sensitivity to the structure of the excited baryon is weak.

The other possible interpretation of the absence of a difference is that in the exclusive experiment the selectivity of the acceptance to the registration of the Δ and N^* decay products might be different. The theoretical consideration of the Δ resonance excitation in $p(p,p)n\pi^+$ reaction and the angular distribution of its decay products performed in [20] support this idea, but the detailed study for the Δ excitation in deuteron is needed.

In Fig. 14 the data for these reaction channels are compared with the existing world data from the inclusive $p(d,d')X$ scattering. A_{yy} of the inclusive data demonstrate an approximate scaling in $|t|$, but the points corresponding to the exclusive measurements are higher than the inclusive ones when taken at about the same beam momentum (p_d =4.5 GeV/c). This feature can be understood if our setup is more selective to the N^* signal, as compared to the inclusive data where a relative contribution of Δ is larger.

V CONCLUSIONS

Tensor and vector analyzing powers for the reactions $dp \to dn\pi^+$, $dp \to dp\pi^0$, $dp \to dN\pi\pi$ were measured in the energy region of the Roper N(1440) resonance excitation as functions of the deuteron 4-momentum transfer squared in the t range, $-0.28 \leq t \leq -0.07$ $(\mathrm{GeV/c})^2$, of the effective mass of the subsystems $(N\pi)$, $(N\pi\pi)$, $1.33 \leq \mathrm{M}_{eff} \leq 1.48$ $\mathrm{GeV/c^2}$, and of the pion emission angle. The results are presented in Table III and in Figs. 10, 12, 14.

The results of this experiment show two interesting features:

- taken as a function of t, one and two pions production channels have the same values of A_{yy} within statistical uncertainty;
- compared to the world data at the nearest beam energy on inclusive $p(d,d')X$, the exclusive A_{yy} data are systematically higher than the inclusive ones when taken at about the same beam momentum.

The simplest possible interpretation of the first point is that the exclusive reaction in the kinematics of this experiment is fully dominated by the Roper. The second point can be explained by hypothesizing that the integration over the full phase space of the missing mass in (d,d') allows some other contribution which lowers A_{yy} somewhat. The Δ comes to mind because it is so overwhelming in this momentum range.

ACKNOWLEDGMENTS

This work was supported in part by INTAS-RFBR grant 95-1345 and by the Russian Foundation for Fundamental Physics Program Grant 122-03. Two participants acknowledge support from the US Department of Energy (V.P., grant N° DE-FG05-89ER40525) and from the US National Science Foundation (C.F.P., grant N° 97-04502). We are thankful for the financial support from IN2P3 and IPN. We are grateful to the staff of the Laboratoire National Saturne (Saclay) and Institut de Physique Nucleaire (Orsay) for the hospitality and support during this work. We thank Prof. A. A. Vorobyov for stimulating discussions and for support in the FS design and construction. We thank Prof. L. S. Azhgirey for fruitful collaborative work and his contribution to the codes used in data analysis. We are thankful to Prof. E. Oset and Dr. S. Hirenzaki for the stimulating discussions and providing us with the program code [21] used for event generation in the period of the preparation of this experiment. We are also very grateful to Prof. M. P. Rekalo for fruitful discussions.

Table III. Spin-dependent observables A_{yy} and A_y.

t (GeV/c)^2	$<\|t\|>$ (GeV/c)^2	θ_π (deg)	A_{yy}	A_y
		$dp \to dn\pi^+$, π^+ is detected in the FS		
	0.22 ± 0.02	$-36^o \le \theta_{\pi^+} \le 6^o$	0.516 ± 0.081	-0.004 ± 0.078
	0.19 ± 0.01	$-36^o \le \theta_{\pi^+} \le 6^o$	0.327 ± 0.046	0.107 ± 0.044
	0.15 ± 0.01	$-36^o \le \theta_{\pi^+} \le 6^o$	0.294 ± 0.032	0.091 ± 0.031
	0.12 ± 0.01	$-36^o \le \theta_{\pi^+} \le 6^o$	0.254 ± 0.037	0.196 ± 0.036
	0.08 ± 0.03	$-36^o \le \theta_{\pi^+} \le 6^o$	0.181 ± 0.066	0.247 ± 0.064
$-0.28 \le t \le -0.14$	0.19 ± 0.05	$0^o \le \theta_{\pi^+} \le 8^o$	0.349 ± 0.062	-0.011 ± 0.06
$-0.28 \le t \le -0.14$	0.19 ± 0.05	$-10^o \le \theta_{\pi^+} \le 0^o$	0.262 ± 0.068	0.051 ± 0.06
$-0.28 \le t \le -0.14$	0.19 ± 0.05	$-38^o \le \theta_{\pi^+} \le -18^o$	0.525 ± 0.083	0.161 ± 0.08
$-0.22 \le t \le -0.1$	0.15 ± 0.05	$0^o \le \theta_{\pi^+} \le 8^o$	0.307 ± 0.056	-0.033 ± 0.055
$-0.22 \le t \le -0.1$	0.15 ± 0.05	$-10^o \le \theta_{\pi^+} \le 0^o$	0.259 ± 0.048	0.130 ± 0.045
$-0.22 \le t \le -0.1$	0.15 ± 0.05	$-38^o \le \theta_{\pi^+} \le -18^o$	0.411 ± 0.065	0.234 ± 0.064
$-0.17 \le t \le -0.07$	0.12 ± 0.05	$0^o \le \theta_{\pi^+} \le 8^o$	0.268 ± 0.079	-0.041 ± 0.072
$-0.17 \le t \le -0.07$	0.12 ± 0.05	$-10^o \le \theta_{\pi^+} \le 0^o$	0.123 ± 0.052	0.197 ± 0.051
$-0.17 \le t \le -0.07$	0.12 ± 0.05	$-38^o \le \theta_{\pi^+} \le -18^o$	0.425 ± 0.098	0.298 ± 0.091
		$dp \to dp\pi^0$, p is detected in the FS		
$-0.28 \le t \le -0.14$	0.19 ± 0.02	$6^o \le \theta_{\pi^0} \le 36^o$	0.428 ± 0.120	-0.204 ± 0.110
$-0.22 \le t \le -0.1$	0.15 ± 0.02	$6^o \le \theta_{\pi^0} \le 36^o$	0.521 ± 0.076	-0.115 ± 0.071
$-0.17 \le t \le -0.07$	0.12 ± 0.02	$6^o \le \theta_{\pi^0} \le 36^o$	0.374 ± 0.065	-0.144 ± 0.061
		$dp \to dN\pi^+\pi$, π^+ is detected in the FS		
	0.22 ± 0.01	$-56^o \le \theta_{\pi^+} \le 0^o$	0.314 ± 0.089	0.031 ± 0.086
	0.19 ± 0.01	$-56^o \le \theta_{\pi^+} \le 0^o$	0.438 ± 0.062	0.005 ± 0.060
	0.15 ± 0.01	$-56^o \le \theta_{\pi^+} \le 0^o$	0.382 ± 0.062	0.048 ± 0.046
	0.12 ± 0.01	$-56^o \le \theta_{\pi^+} \le 0^o$	0.259 ± 0.062	0.053 ± 0.060
	0.08 ± 0.03	$-56^o \le \theta_{\pi^+} \le 0^o$	0.21 ± 0.17	-0.10 ± 0.16
		$dp \to dp\pi\pi$, p is detected in the FS		
	0.22 ± 0.01	$-60^o \le \theta_{\pi(-,+,0)} \le 60^o$	0.351 ± 0.054	0.026 ± 0.048
	0.19 ± 0.01	$-60^o \le \theta_{\pi(-,+,0)} \le 60^o$	0.373 ± 0.038	0.046 ± 0.036
	0.15 ± 0.01	$-60^o \le \theta_{\pi(-,+,0)} \le 60^o$	0.317 ± 0.028	0.036 ± 0.026
	0.12 ± 0.01	$-60^o \le \theta_{\pi(-,+,0)} \le 60^o$	0.250 ± 0.028	0.036 ± 0.027
	0.08 ± 0.03	$-60^o \le \theta_{\pi(-,+,0)} \le 60^o$	0.193 ± 0.050	0.005 ± 0.048

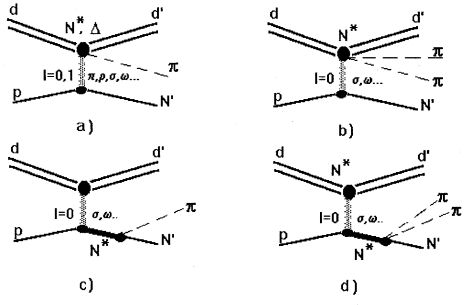

Figure 1: Basic diagrams contributing to $p(d,d')N\pi(\pi)$ reaction a) Δ or N^* resonance excitation "in the deuteron"; b) Roper excitation in the deuteron; c), d) Roper excitation in the target.

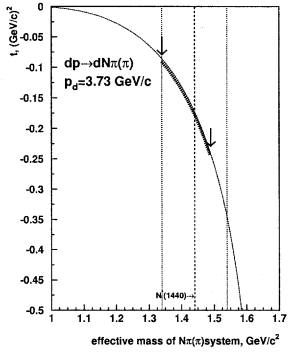

Figure 2: The missing mass M_x (the effective mass N $\pi(\pi)$) versus 4-momentum transfer $|t|$ at the deuteron beam momentum of 3.73 GeV/c. The dashed area represents the region covered in this experiment.

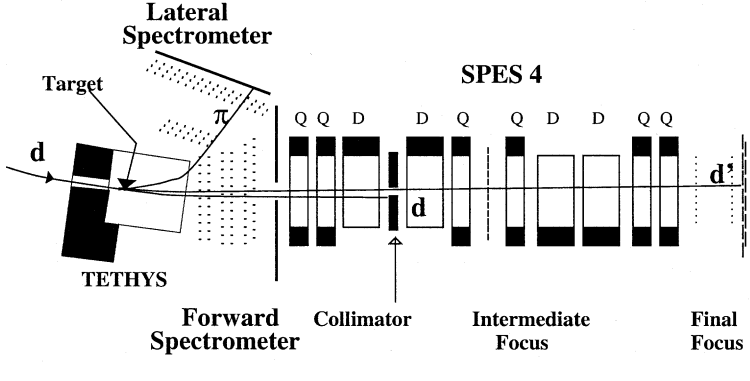

Figure 3: SPES4-π setup.

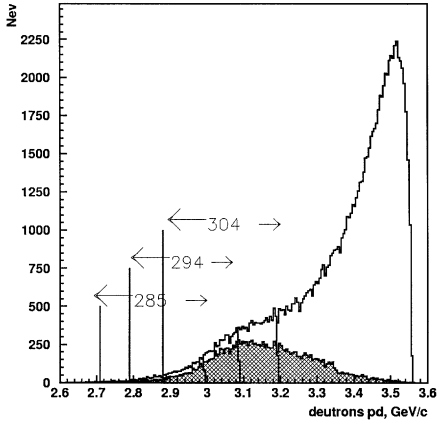

Figure 4: Momentum spectrum of the scattered deuterons. The distribution is generated according with [21]. Regions, covered by the setup acceptance corresponding to the different spectrometer settings, with the central momenta of scattered deuterons of 2.85 GeV/c, 2.94 GeV/c and 3.04 GeV/c are indicated. Dashed region corresponds to the Roper resonance excitation.

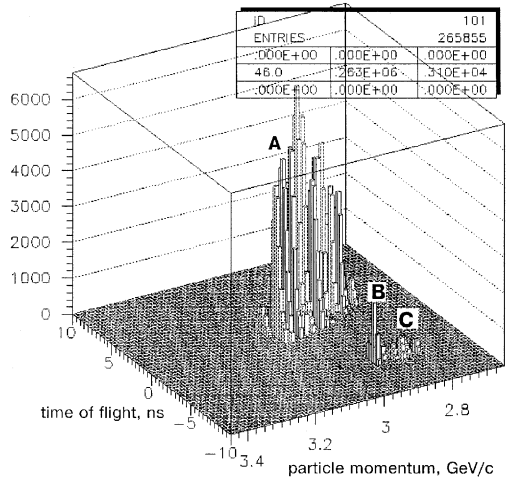

Figure 5: Experimental plot of "momentum in SPES4" (GeV/c) – "time of flight in SPES4" (ns). A: deuterons in the SPES4 from inelastic p(d, d') (the big "mountain"), B: protons from p(d, p)d (the small peak), C: protons from the p(d, p)pn reactions (the tail of the small peak). These regions are well separated.

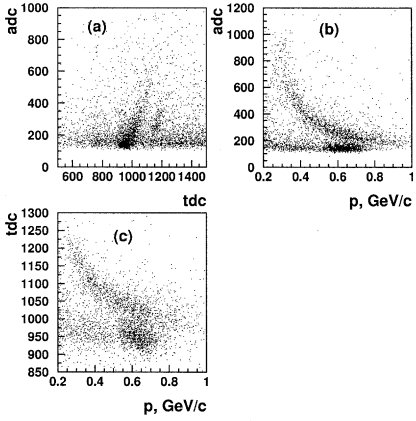

Figure 6: The plots for the particle identification for the FS hodoscope counter number 3 at the SPES4 setting 2.94 GeV/c. a) time of flight (TDC) versus amplitude (ADC) in the FS counter, both in arbitrary units. b) ADC versus the charged particle momentum. c) TDC versus the charged particle momentum.

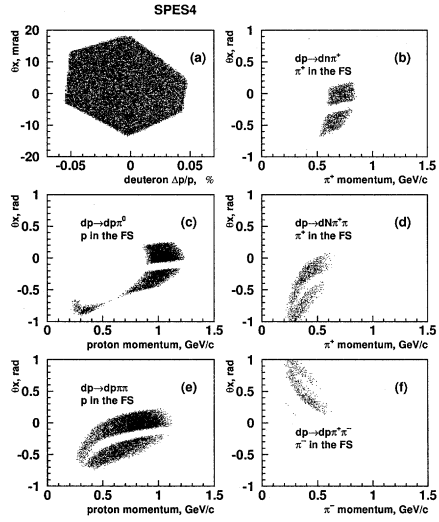

Figure 7: Acceptance of the setup for different reaction channels, calculated using GEANT package. d' is accepted by the SPES4. Events were generated by phase space simulation code GENBOD. a) Momentum versus the horizontal emission angle of deuterons accepted by the SPES4. b), c), d), e), f) Momentum versus the horizontal emission angle of the charged particle from $dp \rightarrow dN\pi(\pi)$ reactions accepted by the FS.

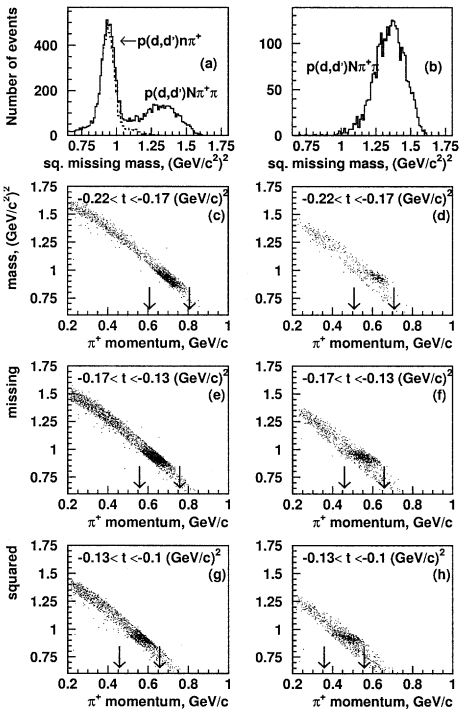

Figure 8: Experimental missing mass squared distributions for $dp \to dN\pi^+(\pi)$ channels when π^+ is detected by the FS at the central momentum of SPES4 equal to 2.94 GeV/c. a) Missing mass squared distribution for all selected events from $dp \to dN\pi^+(\pi)$. Dotted line corresponds to the events from $dn\pi^+$. b) Missing mass squared distribution for events from $dN\pi^+\pi$. The pictures (c, d, e, f, g) represent the missing mass squared versus momentum of π^+ distributions for different intervals of t. The pictures (c, e, h) represent the distributions for the left part of the X-chambers; the pictures (d, f, g) represent the distributions for the right one. The cuts on the momentum of π^+ for the selection of events from $dn\pi^+$ were chosen for each interval of t and for each part of the X-chambers separately (solid arrows in the Figs.(c, d, e, f, g, h)).

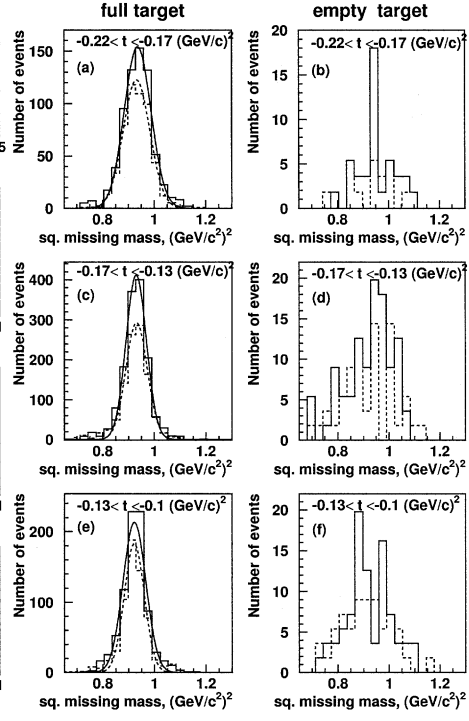

Figure 9: Experimental missing mass squared distributions for $dp \to dn\pi^+$ channel when π^+ is detected by the FS at the central momentum of SPES4 equal to 2.94 GeV/c. Solid line: the positive tensorial polarisation of the beam; dashed line: the negative tensorial polarisation.

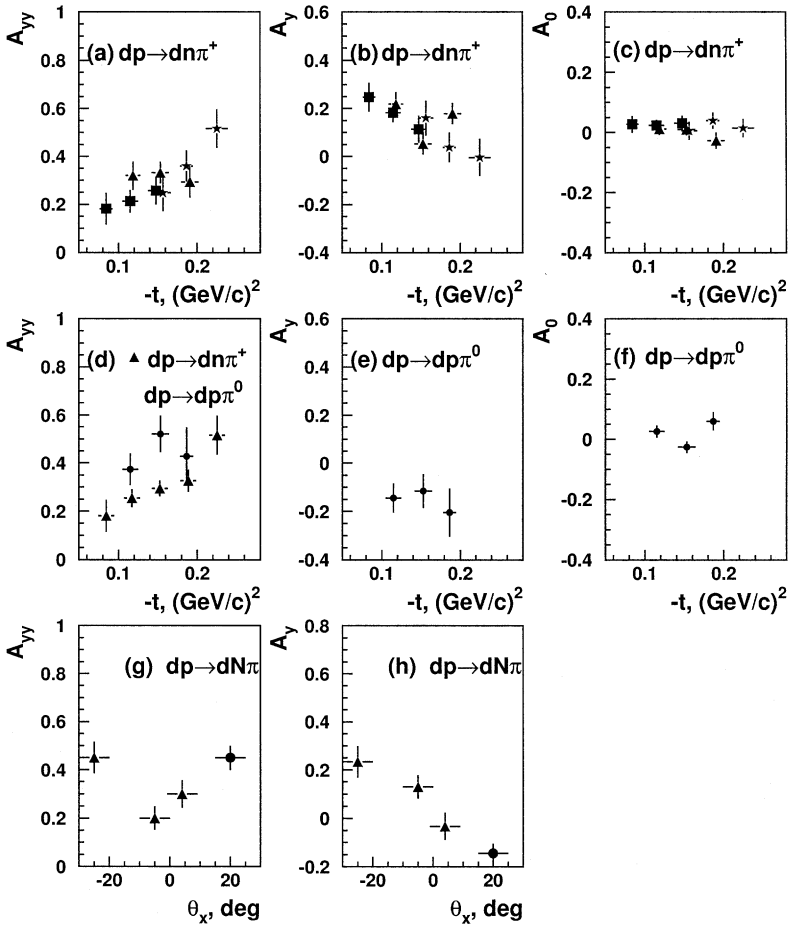

Figure 10: Data for the spin-dependent observables A_{yy} and A_y versus t and θ_π for one pion production channels. Squares: the setting corresponding to the central momentum of SPES4 3.04 GeV/c; triangles: 2.94 GeV/c; stars: 2.85 GeV/c; a) Tensor analyzing power A_{yy} versus $|t|$, for each setting separately. b) Vector analyzing power A_y versus $|t|$, for each setting separately. c) False assymmetry A_0 versus $|t|$, for each setting separately. d) Mean values of A_{yy} for $dn\pi^+$, π^+ detected by the FS (triangles); A_{yy} for $dp\pi^0$, p detected by the FS (filled circles). e) Vector analyzing power A_y for $dp\pi^0$ channel. f) False asymmetry A_0 for $dp\pi^0$ channel. g) Mean values of A_{yy} for $dn\pi^+$ (triangles) and A_{yy} for $dp\pi^0$ (filled circles) versus the horizontal emission angle of the pion in the lab. system. h) Mean values of A_y for $dn\pi^+$ (triangles) and A_y for $dp\pi^0$ (filled circles) versus the horizontal emission angle of the pion in the lab. system.

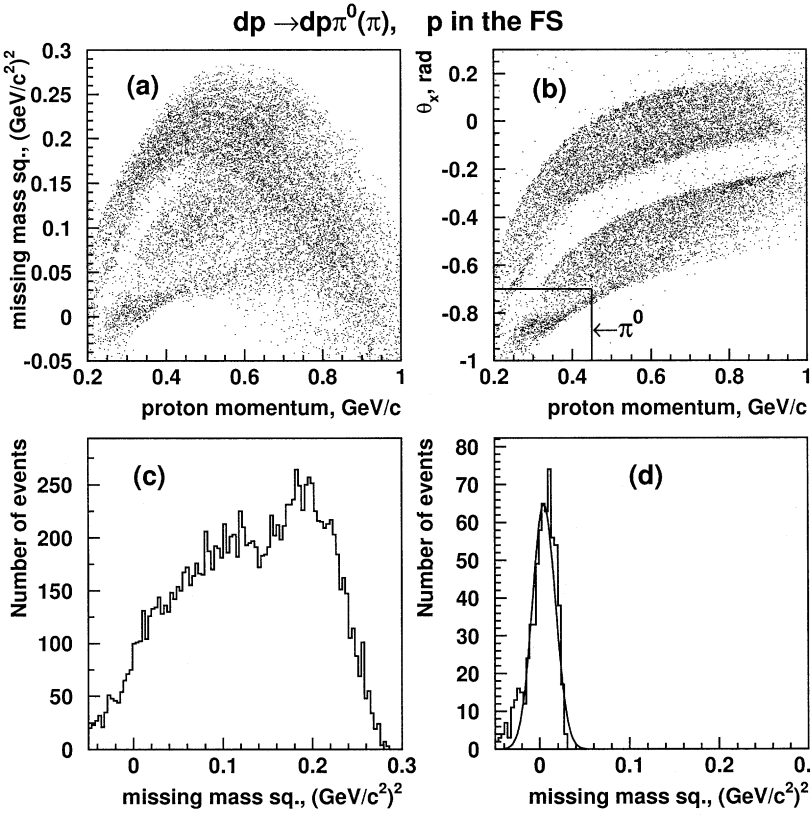

Figure 11: Experimental distributions for $dp \rightarrow dp\pi(\pi)$ reaction, when the protons were registered in the FS at the central momentum of SPES4 equal 2.94 GeV/c. a) Missing mass squared versus the proton momentum. b) Horizontal emission angle versus the proton momentum. c) The missing mass squared for $dp \rightarrow dp\pi(\pi)$ reaction (without cuts). d) The missing mass squared of π^0.

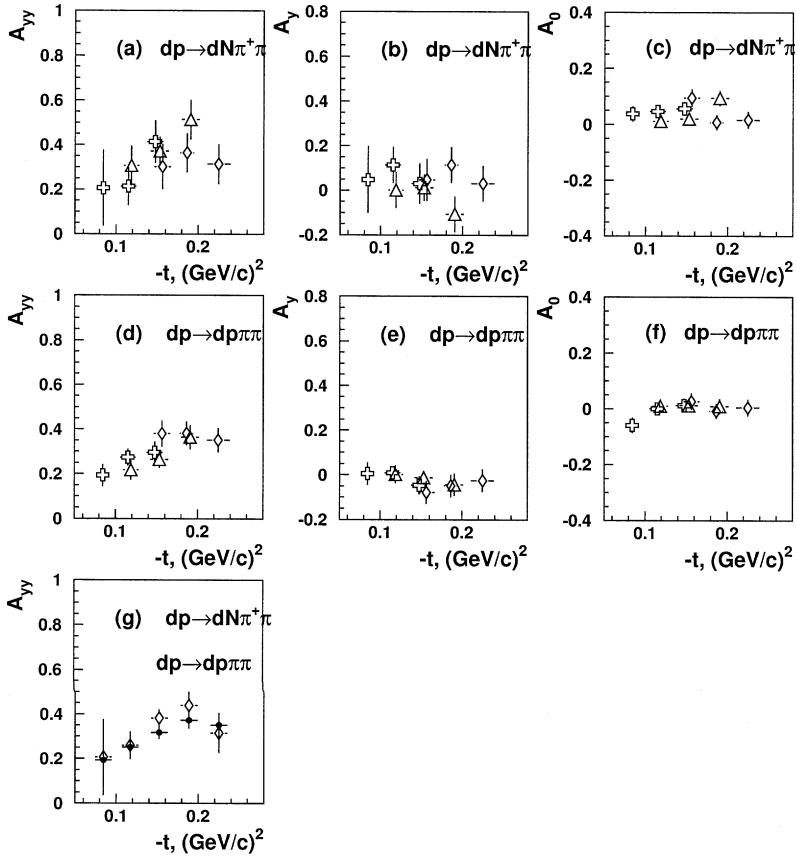

Figure 12: Data on the spin-dependent observables A_{yy}, A_y and A_0 for two-pion final states. In all the panels: Squares: the setting corresponding to the central momentum of SPES4 3.04 GeV/c; triangles: 2.94 GeV/c; stars: 2.85 GeV/c; a), b), c) for $dN\pi^+\pi$, when π^+ is detected by the FS. a) Tensor analyzing power A_{yy}. b) Vector analyzing power A_y. c) False assymetry A_0. d) , e), f) for $dp\pi\pi$, when p detected by the FS. d) Tensor analyzing power A_{yy}. e) Vector analyzing power A_y. f) False assymetry A_0. g) Mean values of A_{yy} for $dN\pi^+\pi$ (empty diamonds), π^+ detected by FS; A_{yy} for $dp\pi\pi$ (filled circles), protons detected by FS.

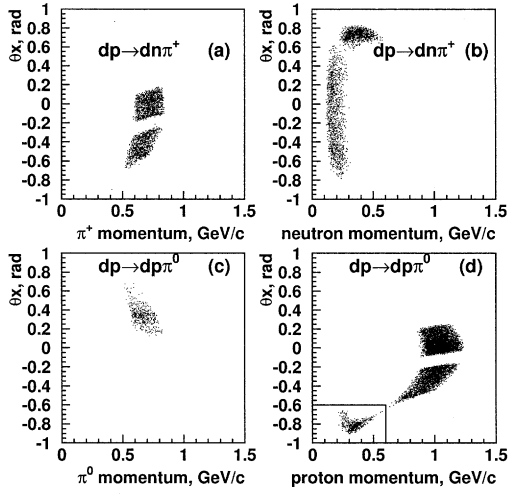

Figure 13: Monte Carlo simulation of the reaction channels: $dp \rightarrow dp\pi^0$; $dp \rightarrow dn\pi^+$: momentum versus the horizontal emission angle of a secondary particle. Events were generated by phase space simulation code GENBOD. Scattered deuterons are accepted by the SPES4.

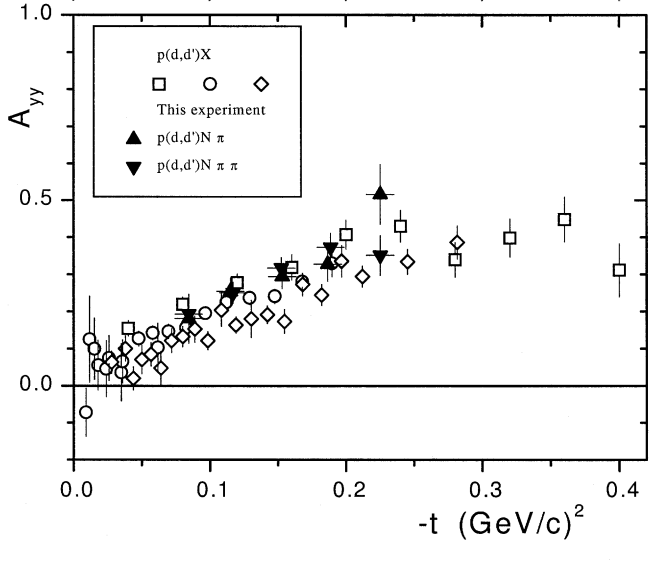

Figure 14:
Comparison of the tensor analyzing power A_{yy} for $\mathrm{p}(d,d')\mathrm{X}$ (world data [6]) with results of this experiment for the reactions $dp \rightarrow dn\pi^+$ and $dp \rightarrow dp\pi\pi$. World data: squares $p_d = 9\ GeV/c$, circles $p_d = 5.5\ GeV/c$, diamonds $p_d = 4.5\ GeV/c$.

References

[1] , L. S. Azhgirey *et al.*, Yad. Fiz. **27**, 1027 (1978); L. S. Azhgirey *et al.*, Yad. Fiz. **30**, 1578 (1979); V. G. Ableev *et al.*, Yad. Fiz. **37**, 348 (1983); L. S. Azhgirey *et al.*, Yad. Fiz. **48**, 1758 (1988).

[2] J. Banaigs *et al.*, Phys. Lett. B **45**, 535 (1973); R. Baldini *et al.*, Nucl. Phys. A **379**, 477 (1982).

[3] Y. Akimov *et al.*, Phys. Rev. Lett. **35**, 763 (1975).

[4] H. P. Morsch *et al.*, Phys. Rev. Lett. **69**, 1336 (1992).

[5] S. Hirenzaki, E. Oset, C. Djalali, M. Morlet, Phys. Rev. C **61**, 044605 (2000).

[6] L. S. Azhgirey *et al.*, Phys. Lett. B **361**, 21 (1995); L. S. Azhgirey *et al.* JINR Rapid Comm., 2[88]-98, 17 (1998).

[7] Data of experiment LNS-250 on Saturne, Saclay, unpublished.

[8] M. P. Rekalo and E. Tomasi-Gustafsson, Phys. Rev. C. **54**, 3125 (1996).

[9] M. P. Rekalo, E. Tomasi-Gustafsson *et al.*, Phys. Rev. C. **59**, 1526 (1999).

[10] V. P. Ladygin *et al.*, Eur. Phys. J. A **8**, 409 (2000).

[11] M.Bedjidian *et al.*, NIM, A**257**, 132 (1987); E.Grorud *et al.*, NIM, A**188**, 549 (1981).

[12] G. D. Alkhazov, A. V. Kravtsov and A. N. Prokofiev, Preprint EP-32-1998 2246, PNPI, Gatchina, (1998) ; A. N. Prokofiev *et al.*, Few Body Systems, Suppl. **10**, 491 (1999) .

[13] L.V Malinina and E.A. Strokovsky, Particles and Nuclei, Lett., **3**[100], 86 (2000).

[14] L. S. Azhgirey *et al.* JINR Rapid Comm., 2[94]-99, 5 (1999); G. D. Alkhazov, A. V. Kravtsov, A. N. Prokofiev, Preprint EP-9-2000, 2352, PNPI, Gatchina, (2000)

[15] Proc. of the 3d Int. Symp. Madison, 1970, ed. by H. H. Barschall, W. Haeberli, Univ. of Wisconsin Press, Madison, WI, 1971.

[16] E.A. Strokovsky *et al.*, Few Body Systems, Suppl. **10**, 495 (1999);
G.D. Alkhazov *et al.*, in Proc. of the XIV International Seminar on High Energy Physics problems (ISHEPP XIV), ed. A.M. Baldin, V.V. Burov, v.II, p.136, Dubna, 2000.

[17] L.S. Azhgirey et al., Phys. Lett. **B391**, 22, (1997); YaF **61**, 494, (1998)

[18] V. Punjabi et al, Phys. Lett. **B350**, 178, (1995)

[19] J. Arvieux *et al.*, Phys. Rev. Lett., **50**, 19 (1983); J. Arvieux *et al.*, Nucl. Phys., A **431**, 1613 (1984).

[20] C. A. Mosbacher, F. Osterfeld Phys. Rev., C**56**, 2014 (1997).

[21] E. Oset, E. Shiino, H. Toki, Phys. Lett., B**224**, 249 (1989); P. Fernandez de Cordoba, E. Oset, Nucl. Phys. A**544**, 793 (1992); P. Fernandez de Cordoba *et al.*, Nucl. Phys. A **586**, 586 (1995).

Received by Publishing Department
on March 6, 2001.

Малинина Л.В. и др. E1-2001-36
Анализирующие способности неупругого dp-рассеяния в области энергий возбуждения дельта-изобары и роперовского резонанса

Изучение неупругого рассеяния поляризованных дейтронов с импульсом 3,73 ГэВ/с на протонах в области энергий возбуждения роперовского резонанса N*(1440) и $\Delta(1232)$ было проведено в эксклюзивном эксперименте с использованием спектрометра SPES4$-\pi$ в Национальной лаборатории SATURNE (Сакле, Франция).

Тензорная и векторная анализирующие способности пионного рождения для реакций $d+p \to d+n+\pi^+$, $d+p \to d+p+\pi^0$, $d+p \to d+N+\pi\pi$ были измерены как функции квадрата переданного четырехимпульса t, эффективной массы подсистем $(N\pi)$, $(N\pi\pi)$ и угла вылета пиона. Наблюдалась сильная зависимость этих анализирующих способностей от угла вылета пиона.

Было обнаружено, что значения A_{yy} для рассматриваемых каналов реакции систематически больше ближайших по энергии пучка известных мировых данных для инклюзивной реакции $p(d,d')X$.

Работа выполнена в Лаборатории высоких энергий ОИЯИ и в Национальной лаборатории SATURNE (Сакле, Франция).

Препринт Объединенного института ядерных исследований. Дубна, 2001

Malinina L.V. et al. E1-2001-36
Analyzing Powers of Inelastic dp-Scattering in the Energy Region of Delta and Roper Resonances Excitation

A study of inelastic scattering of polarized 3.73 GeV/c deuterons on protons in the energy region of the Roper N* (1440) and the $\Delta(1232)$ resonances excitation has been performed in an exclusive experiment at LNS (Laboratoire National SATURNE, Saclay, France) using the SPES4$-\pi$ setup.

Tensor and vector analyzing powers of pion production for the reactions $d+p \to d+n+\pi^+$, $d+p \to d+p+\pi^0$, $d+p \to d+N+\pi\pi$ have been measured as functions of the squared deuteron 4-momentum transfer t, of the effective mass of the subsystems $(N\pi)$, $(N\pi\pi)$ and of the pion emission angle. A strong dependence of these analyzing powers upon the pion emission angle is observed.

It is found that A_{yy} values for the considered reaction channels are systematically larger than the known inclusive $p(d,d')X$ world data at the nearest beam energy.

The investigation has been performed at the Laboratory of High Energies, JINR and at the LNS (Laboratoire National SATURNE, Saclay, France).

Preprint of the Joint Institute for Nuclear Research. Dubna, 2001

Макет Т.Е.Попеко

Подписано в печать 28.03.2001
Формат 60 × 90/16. Офсетная печать. Уч.-изд. листов 2,17
Тираж 425. Заказ 52564. Цена 2 р. 60 к.

Издательский отдел Объединенного института ядерных исследований
Дубна Московской области